### Title

Thermal thresholds heighten sensitivity of West Nile virus transmission to changing temperatures in coastal California




### Journal

Proceedings of the Royal Society B, 287(1932)

### ISSN

0962-8452



### Authors

Skaff, Nicholas K
Cheng, Qu
Clemesha, Rachel ES
et al.



### Publication Date

2020-08-12

### DOI

10.1098/rspb.2020.1065

Peer reviewed

PROCEEDINGS B

royalsocietypublishing.org/journal/rspb

Research

**Cite this article:** Skaff NK *et al*. 2020 Thermal thresholds heighten sensitivity of West Nile virus transmission to changing temperatures in coastal California. *Proc. R. Soc. B* **287**: 20201065.
http://dx.doi.org/10.1098/rspb.2020.1065

Received: 8 May 2020
Accepted: 13 July 2020

**Subject Category:**
Ecology

**Subject Areas:**
health and disease and epidemiology, ecology

**Keywords:**
West Nile virus, temperature, thermal thresholds, climate vulnerability, California, vector-borne disease

**Author for correspondence:**
Justin V. Remais
e-mail: jvr@berkeley.edu

Electronic supplementary material is available online at https://doi.org/10.6084/m9.figshare.c.5077709.

THE ROYAL SOCIETY PUBLISHING

# Thermal thresholds heighten sensitivity of West Nile virus transmission to changing temperatures in coastal California

Nicholas K. Skaff[1], Qu Cheng[1], Rachel E. S. Clemesha[3], Philip A. Collender[1], Alexander Gershunov[3], Jennifer R. Head[2], Christopher M. Hoover[1], Dennis P. Lettenmaier[4], Jason R. Rohr[5], Robert E. Snyder[6] and Justin V. Remais[1]

[1]Division of Environmental Health Sciences, School of Public Health, and [2]Division of Epidemiology, School of Public Health, University of California, Berkeley, CA 94720, USA
[3]Scripps Institution of Oceanography, University of California, San Diego, La Jolla, CA 92037, USA
[4]Department of Geography, University of California, Los Angeles, CA 90095, USA
[5]Department of Biological Sciences, Eck Institute for Global Health, and Environmental Change Initiative, University of Notre Dame, Notre Dame, IN 46556, USA
[6]California Department of Public Health, Vector-Borne Disease Section, Sacramento, CA 95814, USA

NKS, 0000-0002-5929-3966; JVR, 0000-0002-0223-4615

Temperature is widely known to influence the spatio-temporal dynamics of vector-borne disease transmission, particularly as temperatures vary across critical thermal thresholds. When temperature conditions exhibit such 'transcritical variation', abrupt spatial or temporal discontinuities may result, generating sharp geographical or seasonal boundaries in transmission. Here, we develop a spatio-temporal machine learning algorithm to examine the implications of transcritical variation for West Nile virus (WNV) transmission in the Los Angeles metropolitan area (LA). Analysing a large vector and WNV surveillance dataset spanning 2006–2016, we found that mean temperatures in the previous month strongly predicted the probability of WNV presence in pools of *Culex quinquefasciatus* mosquitoes, forming distinctive inhibitory (10.0–21.0°C) and favourable (22.7–30.2°C) mean temperature ranges that bound a narrow 1.7°C transitional zone (21–22.7°C). Temperatures during the most intense months of WNV transmission (August/September) were more strongly associated with infection probability in *Cx. quinquefasciatus* pools in coastal LA, where temperature variation more frequently traversed the narrow transitional temperature range compared to warmer inland locations. This contributed to a pronounced expansion in the geographical distribution of human cases near the coast during warmer-than-average periods. Our findings suggest that transcritical variation may influence the sensitivity of transmission to climate warming, and that especially vulnerable locations may occur where present climatic fluctuations traverse critical temperature thresholds.

## 1. Introduction

Temperature is a fundamental determinant of both vector and parasite fecundity, development and survival, and there are widespread theoretical, observational and experimental studies indicating its role in the transmission of infectious agents [1–4]. In some disease systems and contexts, temperature can exert strong effects over narrow ranges, suggesting that even small fluctuations—resulting from microclimatic conditions or otherwise unremarkable monthly or interannual anomalies—may generate pronounced spatial or temporal heterogeneity in transmission dynamics [5–7]. The influence of such 'transcritical variation', in which values traverse a critical temperature range, may be masked at coarse spatial or temporal scales [8–10], reinforcing the need for

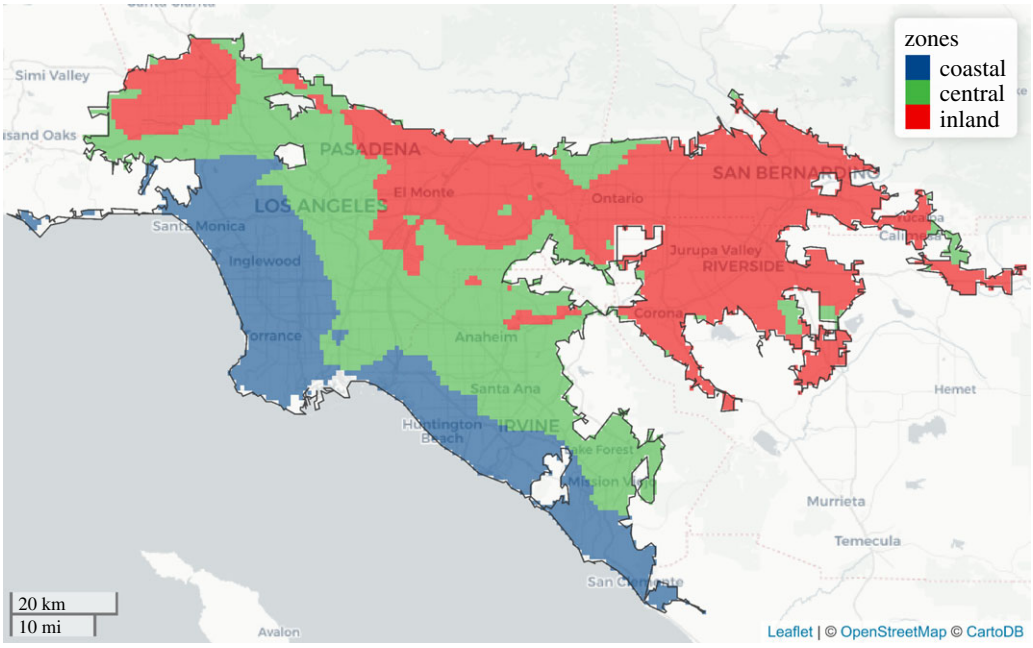


**Figure 1.** Delineation of three climate zones in metropolitan Los Angeles determined by clustering (*k*-means) of average June–October daily mean temperatures over the study period (2006–2016): coastal zone (19.6–22.0°C; blue), central zone (greater than 22.0–23.3°C; green) and inland zone (greater than 23.3–25.4°C; red). The black outline identifies the boundary of metropolitan Los Angeles. (Online version in colour.)

fine-scale analysis of such phenomena to decipher current transmission dynamics and estimate the local and regional implications of climate change.

West Nile virus (WNV, family *Flaviviridae*, genus *Flavivirus*) primarily circulates between *Culex* (*Cx.*) mosquitoes and passerine birds. Though humans are dead-end hosts, WNV is the most common mosquito-borne human pathogen in North America, having infected an estimated 7 million individuals in the United States (US) from 1999 to 2016 [11,12]. The Los Angeles (LA) metropolitan area has reported approximately half of all human WNV disease cases in California [13,14], and has experienced consistent summer and fall transmission since the pathogen emerged in the state in 2003 [13,15]. Many WNV and WNV-vector traits are sensitive to temperature, including virus infection, dissemination and transmission kinetics [16–18], as well as vector fecundity [19,20], feeding rate [19] and longevity [19,20]. Laboratory studies exploring thermal responses of WNV and its vectors, including *Cx. quinquefasciatus*, have informed 'trait-based' mechanistic models yielding estimated lower and upper thresholds for WNV transmission at approximately 20°C and 30°C, respectively, with the optimum temperature ranging from 24°C to 27°C [21–23].

These estimates have yielded crucial information concerning WNV seasonality, broad spatial transmission patterns and expected geographical shifts associated with climate change, but flexible machine learning models developed in data-rich settings can provide new insight into the drivers of sub-annual and geographically localized patterns in disease transmission [4,24,25]. Expanding on laboratory-derived vector-trait thermal response functions, machine learning approaches can accommodate vector and pathogen responses to weather variability at short time scales, such as diurnal temperature cycles and inter-daily temperature fluctuations. Such variation may regulate important physiological processes relevant to WNV transmission [26,27], in part because vector-trait thermal responses are nonlinear and subject to Jensen's inequality—variation can lead to higher or lower transmission than would otherwise be expected under constant temperatures [4,28]. Additionally, machine learning can easily accommodate a large number of biotic and abiotic spatio-temporal transmission determinants simultaneously, like vector larval habitats, the distribution of hosts [29–31] and important interactions between these variables [32], which ultimately determine realized vector and pathogen distributions [10,33]. Exhaustive incorporation of observed meteorological variation—along with the local biotic/abiotic context—would enable the assessment of the influence of transcritical variation on localized heterogeneity in WNV transmission dynamics and vulnerability to climate warming.

We do so here for the LA metropolitan area, developing a spatio-temporal machine learning approach to estimate the nonlinear marginal effects of temperature on WNV infection in the mosquito vector *Cx. quinquefasciatus*. We incorporate measures of average, minimum and maximum temperatures at daily, weekly, monthly and quarterly timescales, along with numerous other climatic and landscape features, to identify thermal thresholds that influence spatio-temporal variation in vector infection. We identify three distinct climate zones in metropolitan L.A. and investigate the effects of temperature on the spatio-temporal dynamics of human WNV incidence across these zones (figure 1). Our results offer new insight into the influence of temperature on the location, timing and intensity of WNV transmission at sub-regional scales, and improve the understanding of how WNV transmission will respond to future climate perturbations.

## 2. Material and methods

### (a) Study area

Metropolitan Los Angeles, as defined here, constitutes three contiguous urban areas delineated by the US Census Bureau: Los Angeles–Long Beach–Anaheim; Riverside–San Bernardino; and Mission Viejo–Lake Forest–San Clemente. The region covers 6368 km$^2$ and has a population of 14 577 039 (2010 census). We

chose this location because: (i) it has the most human WNV cases in California; (ii) vector and pest control agencies in the area conduct and maintain detailed records of extensive vector surveillance activities; and (iii) there is substantial spatio-temporal temperature variability. We grouped metropolitan LA into three zones based on mean temperature values during the typical enzootic WNV transmission season in the region (June–October) using *k*-means clustering. We designate the resulting areas as coastal (19.6–22.0°C mean June–October temperature), central (greater than 22.0–23.3°C) and inland (greater than 23.3–25.4°C) zones (figure 1).

## (b) Mosquito surveillance and human health data

Mosquito surveillance data were acquired via a request to the California Vector-borne Disease Surveillance System (CalSurv), which collects data from more than 50 vector control agencies in California. These data were subsetted to include only adult female *Cx. quinquefasciatus* surveillance records within metropolitan L.A. from 2006 to 2016 that were collected using a single $CO_2$ ($n = 7162$ trap nights) or gravid ($n = 29\,308$ trap nights) trap that was operated for one night without malfunctioning (totalling $n = 36\,470$ trap nights; see additional details in electronic supplementary material, section SI-4). From this, we calculated the number of female *Cx. quinquefasciatus* captured per trap night at each surveillance location ($n = 928$ sites). *Cx. tarsalis*, a highly competent WNV vector common in rural agricultural and wetland habitats of Southern California [34], was infrequently collected across our highly urbanized study area and WNV was rarely detected in the *Cx. tarsalis* pools that were collected, and thus was excluded from analyses. Among all the surveillance records for these two species, 94% (1 806 675 individuals) of the total number of captured mosquitoes and 98% (5731 pools) of all the WNV positive pools were obtained from *Cx. quinquefasciatus* samples.

The onset date and hospitalization date of human West Nile non-neuroinvasive and neuroinvasive disease cases ($n = 2161$) that occurred from 2006 to 2016 in each LA census tract, including cases from Los Angeles, Orange, Riverside and San Bernardino counties, were analysed in partnership with the California Department of Public Health (CDPH), pursuant to CalProtects (Committee for the Protection of Human Subjects) proposal number 17–05–2993, pursuant to the California Civil Code, Article 6, 1798.24. Cases were attributed to each of the three LA climate zones by identifying the zone that contained the centroid of the census tract where the infected individual resided (raster package in R v.3.5.1; see additional details in electronic supplementary material, section SI-4).

## (c) Climate and land cover data

Climate and land cover data, including gridded daily temperature (minimum, maximum; 800 m resolution), gridded daily total precipitation (4 km resolution), gridded daily drought status (as total column soil moisture and as anomalies in total column soil moisture; approx. 6 km resolution), gridded forest canopy cover (30 m resolution), gridded impervious cover (30 m resolution), gridded elevation (10 m resolution) and vectorized wetland cover (delineations from greater than or equal to 1 : 40 000 scale aerial imagery) were acquired from public data sources (see electronic supplementary material, table S3, section SI-5 for data sources, acquisition, attributes and processing details). Several additional gridded variables were derived from the above datasets using raster arithmetic, including daily mean temperature (calculated as the average of daily minimum and maximum temperature), and diurnal variation (difference between daily maximum and minimum temperature). Spatial predictors were estimated within radial buffers (10, 100 and 1000 m) surrounding mosquito surveillance sites and temporal predictors were aggregated (daily, weekly, monthly, quarterly) and lagged to generate several additional predictors (see electronic supplementary material, section SI-5 for details).

## (d) Data analysis

We developed a random forest model predicting the probability of WNV infection in adult female *Cx. quinquefasciatus* pools (hereafter '*Cx.* infection probability') based on the lagged climate and buffered land cover variables detailed above, as well as the total number of female *Cx. quinquefasciatus* captured per trap on the collection day, the number of female *Cx. quinquefasciatus* pooled and tested for WNV (which was occasionally less than the total number of *Cx. quinquefasciatus* captured), and spatial (latitude, longitude) and temporal (year, month, week) features to account for unmeasured confounders that could influence seasonal, interannual and spatial trends, as well as dummy variables for vector control agency and trap type (electronic supplementary material, table S3). We included predictors for vector control agency and trap type, because systematic differences in WNV detection probability due to trap type or in the surveillance priorities of vector control agencies (e.g. trap placement in high-risk areas versus random placement) could introduce significant spatial or temporal bias.

We modelled WNV presence/absence in *Cx. quinquefasciatus* pools as the outcome variable using a random forest classifier, which is a machine learning algorithm that fits many individual classification trees to separate bootstrap samples of a training dataset [35]. Model predictions were generated from an ensemble of the predictions of each tree. This method makes no assumptions about the underlying structure of the data or the relationships between predictors and response, thus accommodating complex spatial and temporal dependence structures, the inclusion of highly collinear predictor variables, and the detection of nonlinear relationships and interactions [36]. Hyperparameter tuning was conducted on a random sample of 20% of the dataset, while out-of-bag validation and blocked cross-validation (spatial and temporal) were conducted on the remaining 80%. These methods were used to estimate overall model error (out-of-bag validation) and error on novel predictions in spatial (mosquito surveillance site) and temporal (yearly and monthly) domains [37], respectively (see electronic supplementary material, section SI-6 for detailed information on random forest model development).

We estimated the relative importance of each predictor variable in order to rank the strength of each variable's influence on *Cx.* infection probability, and to identify climate variables likely responsible for local disparities in transmission. This was accomplished using two separate methods: (i) the change in Gini impurity criterion due to a predictor averaged over all trees; and (ii) the change in overall prediction error associated with permuting the data values of the predictor averaged over all trees [38]. To determine the direction and magnitude of the effects of each predictor variable across the range of predictor variable values, marginal effects of each predictor were estimated as feature contributions, the summed local increments across all nodes split by the predictor (i.e. the change in *Cx.* infection probability due to splits by an individual predictor) averaged over all trees using the forestFloor package in R v.3.5.1 [39]. To minimize overfitting, only out-of-bag observations were used to estimate the marginal effects [39].

We estimated the influence of monthly mean temperature on human WNV cases as mediated by *Cx.* infection probability, and determined if the mediation effect differed between climate zones. First, we used multiple linear regression (equation (2.1)) to evaluate the influence of monthly mean temperature, $T$, on the mediator, average monthly *Cx.* infection probability, $p_i$, modified by metropolitan LA climate zone (coastal, central, inland), Z. The coefficient associated with the interaction between Z and $T$ enabled

us to identify meaningful differences in the effect of monthly mean temperature between zones. Separate models were generated for the July/October and August/September periods, because we anticipated that the effects of temperature would be different during cooler (July/October) and warmer (August/September) periods of the transmission season.

Next, we evaluated whether temperature had a different influence on human WNV incidence between zones during these two time periods. We conducted a moderated mediation analysis and modelled monthly human WNV incidence in each zone as arising from a conditional negative binomial distribution using the medflex package in R v.3.5.1 (equation (2.2)). This analysis enabled the decomposition of the 'total causal effects' of temperature into an indirect component operating through *Cx.* infection probability and direct component acting directly on human WNV incidence. The purpose of this analysis was to separate temperature influences that might directly act on human WNV incidence due factors such as human behaviour, and those operating indirectly through *Cx. quinquefasciatus* infection that would be sensitive to threshold relationships between temperature and *Cx.* infection probability. Mediation effects were calculated by fitting natural effect models, which allowed for separate parameterization of direct and indirect path-specific coefficients within a negative binomial generalized linear model and have the advantage of producing more easily interpretable estimates compared to other mediation and structural equation models [40]. We identified the direct relationship between $T$ and monthly human WNV cases, $H_i$, and the indirect relationship between $T$ and $H_i$ operating through *Cx.* infection probability separately for each metropolitan LA climate zone. An offset was used to account for differences in the human population size, $Po$, of each metropolitan LA climate zone. Climate zone population data were acquired by summing the US Census Bureau estimated 2010 population of all census blocks within each zone. Each $\beta$ coefficient in equation (2.2) represents the natural logarithm of the incidence rate ratio associated with a one unit change in each covariate.

$$p_i = \beta_0 + \beta_2 T + \beta_3 Z + \beta_4 T{*}Z + \varepsilon_1 \quad (2.1)$$

$$\log H_i = \beta_5 + \beta_6 T + \beta_7 Z + \beta_8 T{*}Z + \beta_9 p_i + \varepsilon_2 + \log(Po). \quad (2.2)$$

# 3. Results

## (a) Model performance/validation

The random forest classifier predicting the probability of WNV presence in pools of *Cx. quinquefasciatus* had very good spatio-temporal acuity, attaining an overall AUC (area under the receiver operating characteristic curve) of 0.88 and achieving sensitivity and specificity of 0.82 and 0.80, respectively. The model had 80% overall accuracy in correctly predicting WNV presence/absence in *Cx. quinquefasciatus* pools. AUC, sensitivity and specificity in spatial cross-validation were similar to overall performance measures, demonstrating robust predictions across space and indicating that performance was not strongly biased by spatial autocorrelation or repeated measures at surveillance sites (electronic supplementary material, table S1). Yearly temporal cross-validation revealed lower sensitivity compared to spatial, monthly and overall cross-validated performance—the model detected 72% of true WNV positive pools in years withheld from the training step (electronic supplementary material, table S1), demonstrating a comparatively limited capacity to make accurate interannual predictions of WNV presence.

## (b) Predictor importance and marginal effects of temperature

The average daily mean of maximum and minimum temperatures one month before mosquito sampling (hereafter 'monthly mean temperature') was strongly associated with the predicted probability of WNV presence in *Cx. quinquefasciatus* pools (*Cx.* infection probability). It was identified as the most important environmental predictor in the random forest model by both Gini and permutation importance metrics, and was at least twice as important as any other environmental predictor (electronic supplementary material, figure S1). Temperature variables aggregated over timescales ranging from weekly to quarterly comprised six of the 10 most important predictors by either metric, and were the most important environmental determinants of *Cx.* infection probability in metropolitan LA. Other important predictors included the total number of *Cx. quinquefasciatus* captured in traps, the number of *Cx. quinquefasciatus* that were pooled and tested for WNV infection, and percent forest cover within a 1000 m buffer surrounding vector surveillance sites.

Monthly mean temperature exhibited sigmoidal marginal effects on *Cx.* infection probability, with strong negative effects at monthly mean temperatures below 21°C (henceforth referred to as the 'inhibitory range'), a zone of abrupt increase in *Cx.* infection probability at intermediate values (transitional range), and a zone of strong positive effects at monthly mean temperatures between 22.7 and 30.2°C ('favourable range'; figure 2*a*). The transitional range, wherein the effects of monthly mean temperature shifted from strongly inhibitory to strongly favourable, was notably narrow at 1.7°C (transitional range: 21.0–22.7°C); transcending this range was associated with a marginal increase in *Cx.* infection probability of 40%. Other temperature predictors had relatively weak main effects, but were interactive with monthly mean temperature. These interactions introduced variability in the relationship between monthly mean temperature and the marginal change in *Cx.* infection probability, though the overall shape of the marginal effects curve remained similar (figure 2*b*). Among observations in which favourable monthly mean temperatures occurred (greater than 22.7°C), those that also had extremely high average diurnal variation (greater than 18°C) in the month prior to sampling tended to have lower expected increases in *Cx.* infection probability than otherwise similar observations, signalling that temperature extremes were associated with slight reductions in transmission (electronic supplementary material, figure S2).

## (c) Spatio-temporal variability in temperature effects

We observed spatial differences in the marginal effects of monthly mean temperature (electronic supplementary material, figure S3). Coastal areas generally had lower monthly mean temperatures than locations further inland, and thus less frequently reached the favourable temperature range during the WNV transmission season, whereas inland areas generally had temperatures in the favourable range throughout the peak transmission months of August and September (electronic supplementary material, figure S3). Temporal trends in the marginal effects of monthly mean temperature varied between coastal, central and inland zones (figure 3*a*). We identified disparities in *Cx.* infection probability of up to 40% between zones in some years, depending on whether temperatures in each

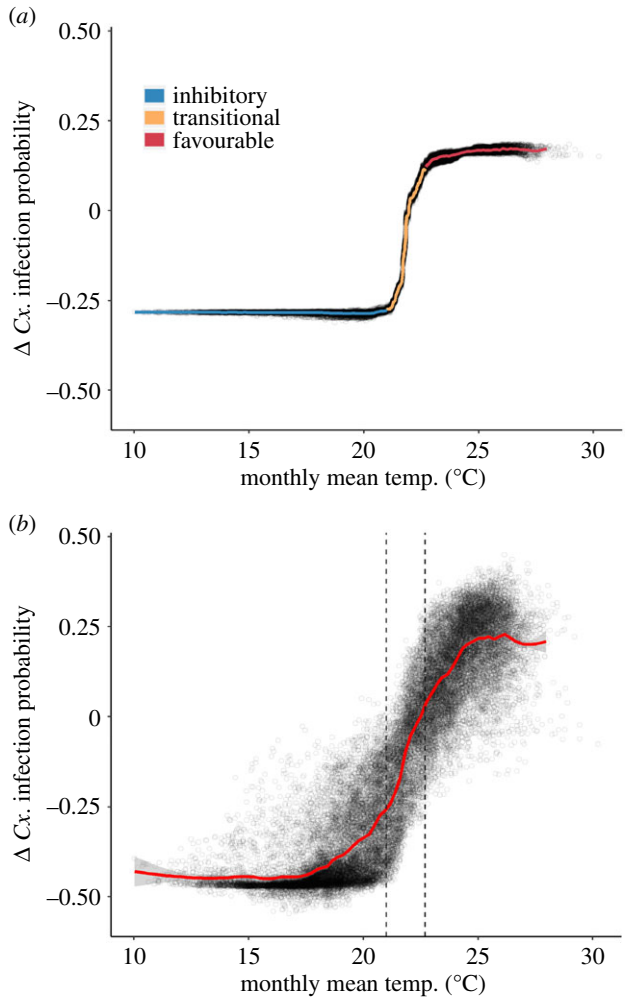


**Figure 2.** Marginal effects plots showing the marginal change in the predicted probability of WNV presence in *Cx. quinquefasciatus* pools (*Cx.* infection probability) associated with: (*a*) monthly mean temperature (with a one-month lag); and (*b*) all temperature predictors in the random forest model (measured at daily, weekly, monthly and quarterly aggregations/lags). Line colour in (*a*) shows inhibitory (blue), transitional (orange) and favourable (red) temperature ranges. Vertical dashed lines in (*b*) highlight the transitional range derived from (*a*). Points in (*a*) and (*b*) represent all observations over the study period. The smoothed marginal effects curves were generated with a generalized additive model. (Online version in colour.)

region crossed the transitional temperature range (electronic supplementary material, figure S4). During anomalously cool years, such as 2011, large differences in the marginal effects of monthly mean temperature emerged between the three zones (figure 3*c*, top): observed monthly mean temperatures in the coastal zone rarely exceeded the inhibitory range, whereas many observations in central and most observations in inland zone reached the favourable temperature range (figure 3*b*, top). In July through October of 2011, 0% of observations in the coastal zone, 38% of observations in the central zone and 79% of observations in the inland zone were in the favourable temperature range. By contrast, during anomalously warm years, such as 2014, similar differences in monthly mean temperatures were observed (figure 3*b*, bottom), yet temperatures generally reached the favourable range across all three—coastal, central and inland—locations, supporting a convergence in *Cx.* infection probability across the region (figure 3*c*, bottom). Thus, transcritical variations in monthly mean temperature were associated with higher variability in *Cx.* infection probability, especially in coastal locations where typical summer mean temperatures spanned the transitional temperature range (figure 3; electronic supplementary material, figure S4).

### (d) Influence of temperature on human WNV incidence mediated by *Cx.* infection probability

Moderated mediation analyses using generalized linear models revealed that monthly mean temperature, operating primarily through changes in *Cx.* infection probability, had a significantly stronger relationship with human WNV incidence in coastal and central than inland zones during the peak WNV transmission season (figure 4; electronic supplementary material, figure S5). From August through September, the most intense months of transmission, the influence of a 1°C monthly mean temperature increase on the percent change in *Cx.* infection probability was stronger in the coastal (6.22 [3.54–8.90 95% CI]) and central zones (5.59 [2.91–8.27 95% CI]) than in the inland zone (2.70 [0.02–5.38 95% CI]; figure 4*a*). Temperature increases mediated through *Cx.* infection probability contributed to significantly higher 1.66 (95% CI 1.33–2.07) and 1.58 (95% CI 1.22–2.04) fold increases in WNV incidence/100 000 persons in coastal and central zones, respectively, than in the inland zone where no statistically significant effects were detected (1.16 [95% CI 0.89–1.51]; figure 4*a*). However, in July and October, cooler months often linked with the rise and the fall of WNV transmission, respectively, the influence of a 1°C monthly mean temperature increase on *Cx.* infection probability was strong in all three zones (figure 4*b*) and was associated with 1.66 (95% CI 1.36–2.02), 1.90 (95% CI 1.50–2.41) and 1.69 (95% CI 1.29–2.21) fold increases in human WNV incidence rates in coastal, central and inland zones, respectively (figure 4*b*).

The differences in the influence of monthly mean temperature on human WNV incidence rates across months and climate zones can be explained by transcritical temperature variation. For instance, directly comparing September 2011, an anomalously cool month, and September 2014, an unusually warm month, we observed that the geographical distribution of WNV cases disproportionately expanded into areas where mean temperatures shifted from transitional to favourable, or all the way from the inhibitory to favourable temperature range (figure 5). Such areas, with monthly temperatures spanning the transitional range, were more likely to exhibit pronounced changes in the human disease burden in response to temperature variation.

## 4. Discussion

We showed how transcritical variation over narrow temperature ranges—often resulting from coastal climate phenomena—can exert an influence on fine-scale spatio-temporal transmission heterogeneity. We found that temperature had strong sigmoidal marginal effects on *Cx.* infection probability across metropolitan Los Angeles, exhibiting a rapid transition from inhibitory to favourable effects over a narrow temperature range (21.0–22.7°C). This relationship, in turn, was associated with geospatial differences in the sensitivity of human WNV incidence to temperature variation. The greatest sensitivity to temperature variation was observed in the coastal zone where temperatures, modulated by cooling marine influences, frequently traversed the inflection point in the marginal effects

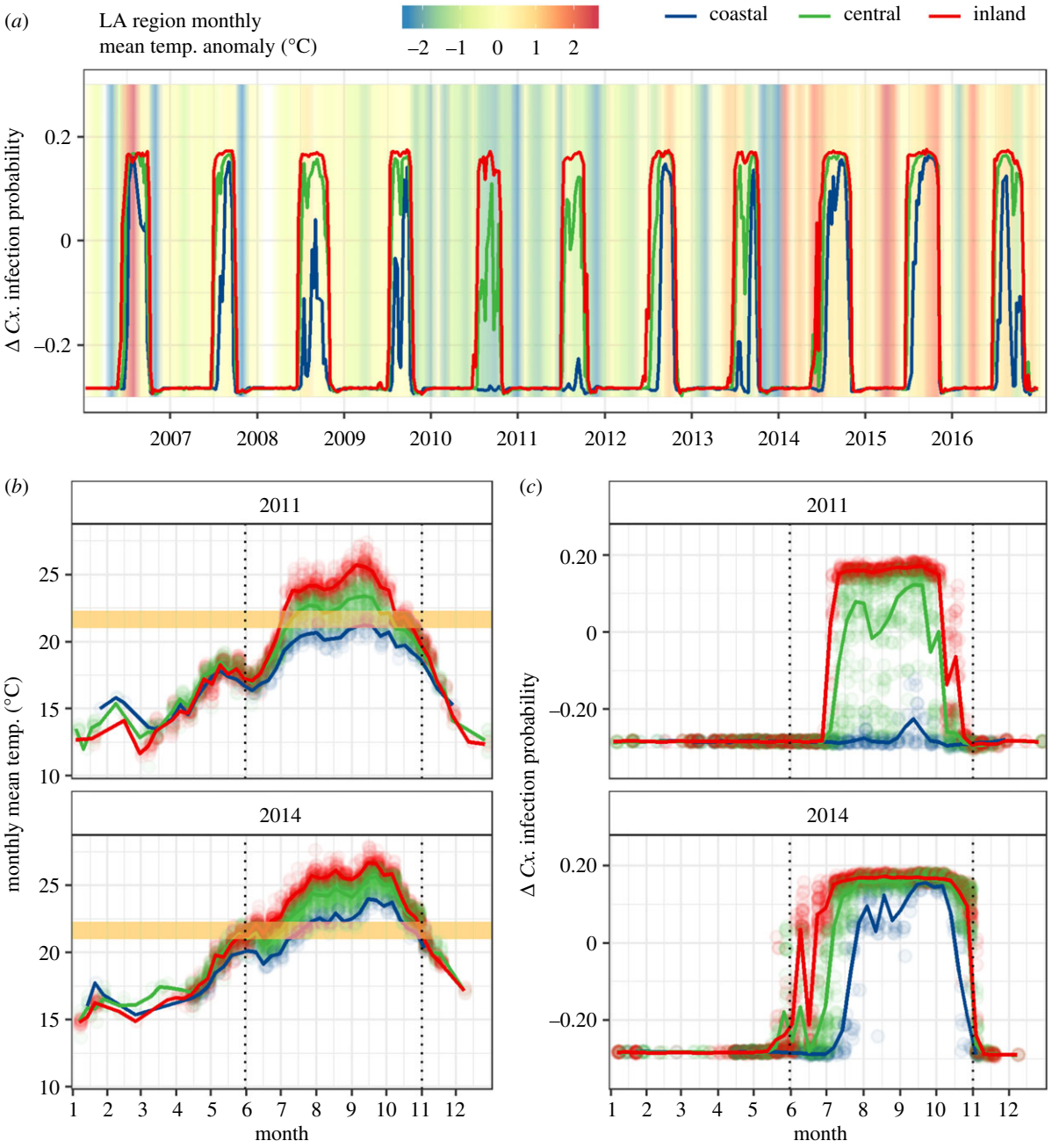


**Figure 3.** Weekly trends in (*a*) the marginal effects of monthly mean temperature on *Cx.* infection probability in each of the three LA climate zones from 2006 to 2016. The background colour in (*a*) shows the average mean monthly temperature anomaly for the entire study area (difference from 2006 to 2016 average for that month). Weekly trends in (*b*) monthly mean temperature and (*c*) the marginal effects of monthly mean temperature on *Cx.* infection probability in an anomalously cool year (2011), and an anomalously warm year (2014) are also shown. The yellow box in (*b*) marks the narrow transitional temperature range (21.0–22.7°C) that lies between inhibitory and favourable temperatures. The dotted vertical lines highlight the months in which transmission typically occurs, June through October. Trend lines represent weekly averages for each region. (Online version in colour.)

curve. Thus, concerns are raised over how transcritical variation may contribute to the sensitivity of disease transmission to future climate warming, potentially exacerbating transmission in key geographical areas.

The sigmoidal relationship between temperature and *Cx.* infection probability is likely the result of temperature sensitivity in several components of the WNV transmission cycle. In particular, the extrinsic incubation period (EIP), or the time between a mosquito's ingestion of an infectious blood meal and its ability to transmit the virus, may drive the upward phase of the curve [16–18]. EIP typically decreases non-linearly with increasing temperature [16–18] and has been shown to be longer in coastal Los Angeles compared to inland areas [18]. Additionally, high temperatures can constrain mosquito abundance by imposing limitations on multiple aspects of the mosquito life cycle, including reproduction, development time, longevity, fecundity and biting rate [19,42]. For example, increasing temperatures are linearly associated with reduced longevity and have threshold or parabolic relationships with egg production, blood feeding and emergence rates of immature *Culex* [19]. Finally, the extreme diurnal temperature variability that was sometimes observed when monthly mean temperatures were very high may have disrupted transmission as temperatures oscillated into an extremely unfavourable range for a short period of time [28]. These phenomena probably contributed to the plateau in *Cx.* infection probability we observed at high temperatures [4,21]. Additional studies that disentangle the interactions between temperature's effects on

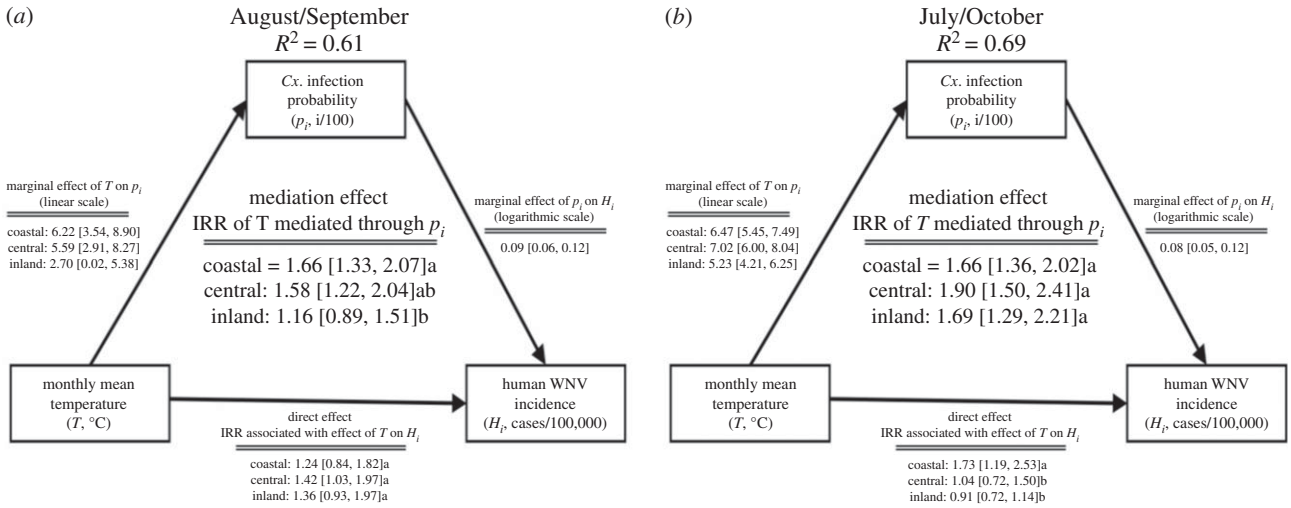


**Figure 4.** Schematic of the mediation model showing the direct effects of average monthly mean temperature on monthly human WNV incidence and the indirect effects mediated by the average monthly *Cx.* infection probability during (*a*) August and September and (*b*) July and October in each metropolitan LA zone. Mediation and direct effect coefficients are incidence rate ratios (IRR), representing the relative increase in incidence attributed to a 1°C increase in monthly mean temperature. Brackets contain 95% confidence intervals and letters show statistically significant differences in mediation and direct effects among metropolitan L.A. zones ($p < 0.05$). Diagram adapted from publicly available R code [41].

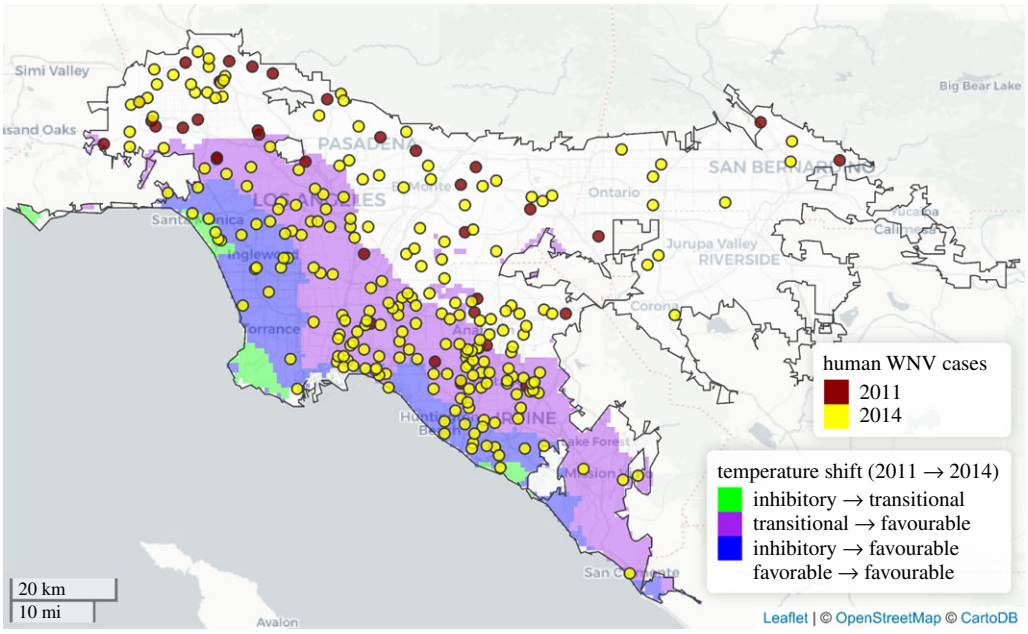


**Figure 5.** Census tract centroids where human WNV cases occurred, geomasked with random displacement within a 20 km × 20 km grid, during a cool period, September 2011 (red points) and a warm period, September 2014 (yellow points). Geographical expansion of cases in 2014 (yellow points) occurred in areas where transcritical variation between the cool and warm period occurred, either from the inhibitory to favourable (blue shading), or from the transitional to favourable (purple shading) temperature range. Areas with no shading within the black metropolitan LA boundary remained in the favourable range for the duration of both time periods. Random displacement of centroids within each grid square was restricted to locations with the same temperature shading as the true centroid. (Online version in colour.)

different vector life-history characteristics could more conclusively identify the mechanistic underpinning of the observed sigmoidal relationship.

As a result of the observed thermal threshold, the sensitivity of WNV transmission to temperature variation was markedly different in the cool coastal zone and the warmer inland zone. In August and September, increases in monthly mean temperature had more pronounced effects on *Cx.* infection probability—and also on human WNV incidence—in the coastal and central zones than inland, whereas in July and October, similar effects on *Cx.* infection probability were detected in all zones. These differences were related to the months in which natural variability in temperature traversed the observed thermal threshold. Inland zones were almost always too warm in August and September, though sometimes cool enough in July and October, to cross the inflection point. Typical mean temperatures in the coastal and central zones were close enough to the threshold that crossing the inflection point was possible from July through October. Thus, the length of the WNV transmission season may be sensitive to temperature variation in all of metropolitan LA, but transcritical variation is most likely to coincide with the occurrence of a transmission season and the maximum intensity of transmission in the cool coastal zones.

Based on these findings, changes in disease transmission due to climate warming—classically conceived as shifting the transmission to higher latitudes or elevations [1,26,43,44]—

may be most intense in zones where present climatic fluctuations most frequently traverse critical temperature thresholds. For instance, global climate models from Climate Model Intercomparison Project version 5 (CMIP5) following Representative Concentration Pathway 4.5 anticipate a 1.26°C mid-century (2040–2069) increase in August–September mean temperature in LA's coastal zone [45], which would push coastal temperatures more consistently into the favourable temperature range for WNV transmission during that period (electronic supplementary material, figures S6 and S7). However, more extreme 1.76°C projected increases in August–September mean temperatures in less-vulnerable inland locations would not substantially change the favourability for WNV transmission according to our model (electronic supplementary material, figures S6 and S7). As warming intensifies, the locations that are most sensitive to increasing temperatures may shift, following the distribution of areas where the new local temperature range abuts key temperature thresholds.

Though laboratory-derived estimates of WNV transmission depict a unimodal thermal response curve with declines in transmission at very high temperatures [21,23], our findings generally show a monotonic relationship with only the slight appearance of diminishing *Cx.* infection probability at the highest diurnal extremes. The mean temperatures in this study may not have sufficiently exceeded the optimal range for transmission in order for declines to be detected. This suggests that our findings, like the findings from many correlative empirical models, are limited in their applicability to 'novel' future climates, especially in hot inland areas where warming is likely to raise temperatures beyond the observed range [46,47]. We also do not address future shifts in precipitation regimes, though changes in the region are expected to be small relative to current variability [48] and precipitation had relatively weak effects in our random forest model compared to temperature. Further, changes in disease transmission due to climate change also depend on an assortment of factors other than thermal optima, such as socioeconomics, behaviour, immunity, vector species composition and vector control activities [2,3,49,50], as well as potential adaptations to changing climate conditions among vectors and pathogens [3,51,52]. Clarifying the role of these phenomena in WNV and other infectious disease systems would be a valuable avenue for research complementing the present work.

We also note that we were unable to account for several factors that may have had an important effect on enzootic and human WNV transmission in the study region. Mosquito control activities, including the applications of larvicides and adulticides, are conducted by five different vector control districts across the study area (electronic supplementary material, section SI-4) and likely varied by district and over fine spatial and temporal scales, but information on such activities was not readily available. Also, passerine birds, which are the primary enzootic host for WNV, exhibit seasonal and multi-year cycles in population size and acquired immunity that were not accounted for in the present analyses [15,53]. The capacity to predict the occurrence of WNV infection in *Culex spp.* and determine the mechanisms by which temperature and other variables influence transmission could be improved in future studies by incorporating records of mosquito control activities and via systematic monitoring of passerine population size and seroprevalence. While temperature is associated with WNV infection in humans, these other factors may have also contributed to interannual variability in human incidence especially in warm inland locations with consistently favourable temperatures.

Here, we found that spatial and temporal variation in temperature across a narrow range of 21–22.7°C was associated with pronounced localized differences in entomological and epidemiological disease risk. Such transcritical temperature variation was linked with greater sensitivity of transmission to temperature increases in the coastal zone, and likely signals vulnerability to future warming that positions this area more frequently in the most favourable temperature range for WNV transmission. Though climate change-driven shifts in pathogen distributions to novel locations have been a consistent research focus and are undoubtedly consequential, our results emphasize that some of the most vulnerable areas may already be situated within coarsely defined endemic zones. These vulnerable locations, like cooler high elevation or coastal climates, may be masked at coarse scales because they constitute relatively small total land areas, but they can contain a disproportionately large proportion of the susceptible human population [10,54] because of their historical status as refuges from disease transmission [54] or as economic hubs [55]. Thus, further research on the concordance between highly susceptible human populations and local climates that are likely to cross critical temperature thresholds could be instrumental in identifying areas and populations at greatest risk, subsequently helping to mitigate the human burden of infectious diseases such as WNV in a changing climate.

Data accessibility. The R script used to conduct the data analysis is available in a publicly accessible GitHub repository (https://github.com/nskaff/Skaff_et_al_WNV_thermal_thresholds). The mosquito surveillance data are publicly accessible by data request to CalSurv [56]. Human case data are protected health information (PHI) with access restricted to authorized California Department of Public Health (CDPH) staff. Limited, deidentified human case data are available via California's Open Data Portal (https://data.ca.gov/). More complete human disease data can be obtained for approved purposes by submitting a formal request to the CPDH, Infectious Diseases Branch, Surveillance and Statistics Section [57]. A dataset containing the environmental predictors included in the random forest and mediation models are posted in a publicly accessible repository on the Knowledge Network for Biocomplexity [58].

Authors' contributions. N.K.S. and J.V.R. designed the research, N.K.S. and P.A.C. analysed the data, R.E.S.C. developed the climate projections, N.K.S., P.A.C., C.M.H., Q.C., J.R.H., P.A.C, R.E.S.C, A.G., D.P.L, J.R.R., R.E.S. and J.V.R. wrote the paper.

Competing interests. The authors declare no competing interests.

Funding. Funding was provided by UC Multicampus Research Programs and Initiatives (MRP award no. 17-446315), NSF Water, Sustainability and Climate program (award nos 1360330 and 1646708), the NSF/NIH Ecology and Evolution of Infectious Diseases program (FIC award no. R01TW010286), NSF grants EF-1241889, DEB-1518681 and IOS-1754868, the NOAA Regional Integrated Sciences and Assessments (RISA) California–Nevada Climate Applications Program (award NA17OAR4310284), the NOAA Coastal and Ocean Climate Applications (COCA) Program (award NA15OAR4310114) and the National Institutes of Health (NIAID award R01AI125842).

Acknowledgements. We thank the individuals and organizations that made this research possible by providing data and support, including the Vector-Borne Disease Section at the California Department of Public Health, the Davis Arboviral Research and Training laboratory, the Mosquito and Vector Control Association of California, as well as local health jurisdictions and vector control agencies that conducted human and environmental WNV surveillance. We also thank the Mordecai Lab, Dr. Hugh Sturrock and the UCSF Spatial Epidemiology Group for their helpful feedback.

## References


1. Patz JA, Epstein PR, Burke TA, Balbus JM. 1996 Global climate change and emerging infectious diseases. *J. Am. Med. Assoc.* **275**, 217–223. (doi:10.1001/jama.1996.03530270057032)
2. Lafferty KD. 2009 The ecology of climate change and infectious diseases. *Ecology* **90**, 888–900. (doi:10.1890/08-0079.1)
3. Altizer S, Ostfeld RS, Johnson PTJ, Kutz S, Harvell CD. 2013 Climate change and infectious diseases: from evidence to a predictive framework. *Science* **341**, 514–519. (doi:10.1126/science.1239401)
4. Mordecai EA *et al*. 2019 Thermal biology of mosquito-borne disease. *Ecol. Lett.* **22**, 1690–1708. (doi:10.1111/ele.13335)
5. Ngowo HS, Kaindoa EW, Matthiopoulos J, Ferguson HM, Okumu FO. 2017 Variations in household microclimate affect outdoor-biting behaviour of malaria vectors. *Wellcome Open Res.* **2**, 102. (doi:10.12688/wellcomeopenres.12928.1)
6. Paaijmans KP, Thomas MB. 2011 The influence of mosquito resting behaviour and associated microclimate for malaria risk. *Malar. J.* **10**, 183. (doi:10.1186/1475-2875-10-183)
7. Pascual M, Ahumada JA, Chaves LF, Rodo X, Bouma M. 2006 Malaria resurgence in the East African highlands: temperature trends revisited. *Proc. Natl Acad. Sci. USA* **103**, 5829–5834. (doi:10.1073/pnas.0508929103)
8. Bejon P *et al.* 2014 A micro-epidemiological analysis of febrile malaria in Coastal Kenya showing hotspots within hotspots. *Elife* **3**, e2130. (doi:10.7554/eLife.02130)
9. Winters AM *et al.* 2010 Spatial risk assessments based on vector-borne disease epidemiologic data: importance of scale for West Nile virus disease in Colorado. *Am. J. Trop. Med. Hyg.* **82**, 945–953. (doi:10.4269/ajtmh.2010.09-0648)
10. Cohen JM *et al.* 2016 Spatial scale modulates the strength of ecological processes driving disease distributions. *Proc. Natl Acad. Sci. USA* **113**, E3359–E3364. (doi:10.1073/pnas.1521657113)
11. Reimann CA *et al.* 2008 Epidemiology of neuroinvasive arboviral disease in the United States, 1999–2007. *Am. J. Trop. Med. Hyg.* **79**, 974–979. (doi:10.4269/ajtmh.2008.79.974)
12. Ronca SE, Murray KO, Nolan MS. 2019 Cumulative incidence of West Nile virus infection, continental United States, 1999–2016. *Emerg. Infect. Dis.* **25**, 325. (doi:10.3201/eid2502.180765)
13. Department of Public Health. 2019 WNV levels elevated in Los Angeles County. See http://publichealth.lacounty.gov/acd/WNVData.htm.
14. Centers for Disease Control. 2018 Final cumulative maps & data for 1999–2016. https://www.cdc.gov/westnile/statsmaps/cumMapsData.html.
15. Kwan JL, Kluh S, Madon MB, Reisen WK. 2010 West Nile virus emergence and persistence in Los Angeles, California, 2003–2008. *Am. J. Trop. Med. Hyg.* **83**, 400–412. (doi:10.4269/ajtmh.2010.10-0076)
16. Kilpatrick AM, Meola MA, Moudy RM, Kramer LD. 2008 Temperature, viral genetics, and the transmission of West Nile virus by *Culex pipiens* mosquitoes. *PLoS Pathog.* **4**, e1000092. (doi:10.1371/journal.ppat.1000092)
17. Dohm DJ, O'Guinn ML, Turell MJ. 2002 Effect of environmental temperature on the ability of *Culex pipiens* (Diptera: Culicidae) to transmit West Nile virus. *J. Med. Entomol.* **39**, 221–225. (doi:10.1603/0022-2585-39.1.221)
18. Reisen WK, Fang Y, Martinez VM. 2014 Effects of temperature on the transmission of West Nile virus by *Culex tarsalis* (Diptera: Culicidae). *J. Med. Entomol.* **43**, 309–317. (doi:10.1093/jmedent/43.2.309)
19. Ciota AT, Matacchiero AC, Kilpatrick AM, Kramer LD. 2014 The effect of temperature on life history traits of Culex mosquitoes. *J. Med. Entomol.* **51**, 55–62. (doi:10.1603/ME13003)
20. Oda T *et al.* 1999 Effects of high temperature on the emergence and survival of adult *Culex pipiens* molestus and *Culex quinquefasciatus* in Japan. *J. Am. Mosq. Control Assoc.* **15**, 153–156.
21. Paull SH *et al.* 2017 Drought and immunity determine the intensity of West Nile virus epidemics and climate change impacts. *Proc. R. Soc. B* **284**, 20162078. (doi:10.1098/rspb.2016.2078)
22. Hartley DM *et al.* 2012 Effects of temperature on emergence and seasonality of West Nile virus in California. *Am. J. Trop. Med. Hyg.* **86**, 884–894. (doi:10.4269/ajtmh.2012.11-0342)
23. Shocket MS *et al*. 2019 Transmission of West Nile virus and other temperate mosquito-borne viruses occurs at lower environmental temperatures than tropical diseases. *bioRxiv* 597898. (doi:10.1101/597898)
24. Parham PE, Michael E. 2010 Modeling the effects of weather and climate change on malaria transmission. *Environ. Health Perspect.* **118**, 620–626. (doi:10.1289/ehp.0901256)
25. Morin CW, Comrie AC. 2013 Regional and seasonal response of a West Nile virus vector to climate change. *Proc. Natl Acad. Sci. USA* **110**, 15 620–15 625. (doi:10.1073/pnas.1307135110)
26. Mills JN, Gage KL, Khan AS. 2010 Potential influence of climate change on vector-borne and zoonoticdiseases: a review and proposed research plan. *Environ. Health Perspect.* **118**, 1507–1514. (doi:10.1289/ehp.0901389)
27. Raffel TR *et al.* 2013 Disease and thermal acclimation in a more variable and unpredictable climate. *Nat. Clim. Change* **3**, 146–151. (doi:10.1038/nclimate1659)
28. Paaijmans KP *et al.* 2010 Influence of climate on malaria transmission depends on daily temperature variation. *Proc. Natl Acad. Sci. USA* **107**, 15 135–15 139. (doi:10.1073/pnas.1006422107)
29. Mbogo CM *et al.* 2003 Spatial and temporal heterogeneity of anopheles mosquitoes and *Plasmodium falciparum* transmission along the Kenyan coast. *Am. J. Trop. Med. Hyg.* **68**, 734–742. (doi:10.4269/ajtmh.2003.68.734)
30. Smith DL, Dushoff J, McKenzie FE. 2004 The risk of a mosquito-borne infectionin a heterogeneous environment. *PLoS Biol.* **2**, e368. (doi:10.1371/journal.pbio.0020368)
31. Lambin EF, Tran A, Vanwambeke SO, Linard C, Soti V. 2010 Pathogenic landscapes: interactions between land, people, disease vectors, and their animal hosts. *Int. J. Health Geogr.* **9**, 54. (doi:10.1186/1476-072X-9-54)
32. Davidson AD, Hamilton MJ, Boyer AG, Brown JH, Ceballos G. 2009 Multiple ecological pathways to extinction in mammals. *Proc. Natl Acad. Sci. USA* **106**, 10 702–10 705. (doi:10.1073/pnas.0901956106)
33. Wisz MS *et al.* 2013 The role of biotic interactions in shaping distributions and realised assemblages of species: implications for species distribution modelling. *Biol. Rev.* **88**, 15–30. (doi:10.1111/j.1469-185X.2012.00235.x)
34. Reisen WK, Barker CM, Fang Y, Martinez VM. 2008 Does variation in culex (Diptera: Culicidae) vector competence enable outbreaks of West Nile virus in California? *J. Med. Entomol.* **45**, 1126–1138. (doi:10.1093/jmedent/45.6.1126)
35. Breiman L. 2001 Random forests. *Mach. Learn.* **45**, 5–32. (doi:10.1023/A:1010933404324)
36. Cutler DR *et al.* 2007 Random forests for classification in ecology. *Ecology* **88**, 2783–2792. (doi:10.1890/07-0539.1)
37. Roberts DR *et al.* 2017 Cross-validation strategies for data with temporal, spatial, hierarchical, or phylogenetic structure. *Ecography* **40**, 913–929. (doi:10.1111/ecog.02881)
38. Boulesteix A-L, Janitza S, Kruppa J, König IR. 2012 Overview of random forest methodology and practical guidance with emphasis on computational biology and bioinformatics:random forests in bioinformatics. *Wiley Interdiscip. Rev. Data Min. Knowl. Discov.* **2**, 493–507. (doi:10.1002/widm.1072)
39. Welling SH, Refsgaard HH, Brockhoff PB, Clemmensen LH. 2016 Forest floor visualizations of random forests. *ArXiv* abs/1605.09196.
40. Steen J, Loeys T, Moerkerke B, Vansteelandt S. 2017 Medflex: an R package for flexible mediation analysis using natural effect models. *J. Stat. Softw.* **76**. (doi:10.18637/jss.v076.i11)
41. Lane D. 2018 R script for plotting simple mediation models. See https://github.com/danslane/MediationPlotter.
42. Rueda LM, Patel KJ, Axtell RC, Stinner RE. 1990 Temperature-dependent development and survival rates of *Culex quinquefasciatus* and *Aedes aegypti* (Diptera: Culicidae). *J. Med. Entomol.* **27**, 892–898. (doi:10.1093/jmedent/27.5.892)
43. Jetten TH, Focks DA. 1997 Potential changes in the distribution of dengue transmission under climate

warming. *Am. J. Trop. Med. Hyg.* **57**, 285–297. (doi:10.4269/ajtmh.1997.57.285)
44. Patz JA, Campbell-Lendrum D, Holloway T, Foley JA. 2005 Impact of regional climate change on human health. *Nature* **438**, 310–317. (doi:10.1038/nature04188)
45. Pierce DW, Kalansky JF, Cayan DR. 2018 *Climate, drought, and sea level rise scenarios for the fourth California climate assessment*. Sacramento, CA: California Energy Commission.
46. Buckley LB *et al.* 2010 Can mechanism inform species' distribution models? *Ecol. Lett.* **13**, 1041–1054. (doi:10.1111/j.1461-0248.2010.01506.x)
47. Williams JW, Jackson ST. 2007 Novel climates, no-analog communities, and ecological surprises. *Front. Ecol. Environ.* **5**, 475–482. (doi:10.1890/070037)
48. Berg N *et al.* 2015 Twenty-first-century precipitation changes over the Los Angeles region. *J. Clim.* **28**, 401–421. (doi:10.1175/JCLI-D-14-00316.1)
49. Rohr JR *et al.* 2011 Frontiers in climate change–disease research. *Trends Ecol. Evol.* **26**, 270–277. (doi:10.1016/j.tree.2011.03.002)
50. Reiter P. 2001 Climate change and mosquito-borne disease. *Environ. Health Perspect.* **109**, 141–161.
51. Hoberg EP, Brooks DR. 2015 Evolution in action: climate change, biodiversity dynamics and emerging infectious disease. *Phil. Trans. R. Soc. B* **370**, 20130553. (doi:10.1098/rstb.2013.0553)
52. Koelle K, Pascual M, Yunus M. 2005 Pathogen adaptation to seasonal forcing and climate change. *Proc. R. Soc. B* **272**, 971–977. (doi:10.1098/rspb.2004.3043)
53. Kilpatrick AM, Kramer LD, Jones MJ, Marra PP, Daszak P. 2006 West Nile virus epidemics in North America are driven by shifts in mosquito feeding behavior. *PLoS Biol.* **4**, e82. (doi:10.1371/journal.pbio.0040082)
54. Lindsay SW, Martens WJ. 1998 Malaria in the African highlands: past, present and future. *Bull. World Health Organ.* **76**, 33–45.
55. McGaugh ME. 1970 *A geography of population and settlement*. Dubuque, IA: WC Brown Company Publishers.
56. CalSurv. 2019 California vectorborne disease surveillance data policy. See https://calsurv.org/assets/files/calsurv_data_policy.pdf.
57. CDPH. 2019 Request for infectious diseases branch surveillance data. See https://public.staging.cdph.ca.gov/sites/ada/CDPH%20Document%20Library/ControlledForms/cdph9078.pdf.
58. Knowledge Network for Biocomplexity. 2019 Thermal thresholds increase the vulnerability of coastal Los Angeles to temperature-linked increases in West Nile virus transmission. See https://knb.ecoinformatics.org/view/doi:10.5063/F13N21QH.